Application of Proper Orthogonal Decomposition to Particulate Processes

Michael Mangold * **Mykhaylo Krasnyk** **

* *Max Planck Institute for Dynamics of Complex Technical Systems, Sandtorstr. 1, 39106 Magdeburg, Germany (Tel: +49-391-6110361; e-mail: mangold@mpi-magdeburg.mpg.de).*
** *Donetsk National Technical University, Faculty of Computer Science and Technology, Donetsk, Ukraine (e-mail: michael.krasnyk@googlemail.com).*

Abstract: Particulate processes like industrial crystallisation or granulation are often described by population balances. This leads to mathematical models containing partial integro differential equations. In many cases, the flow conditions of the fluid phase have a strong impact on the particle formation. To describe this properly, Navier Stokes equations have to be solved in addition. The resulting model equation system is too complicated to apply them to typical process control tasks. Reduced models are desirable. In this contribution, the use of proper orthogonal decomposition is suggested as a powerful reduction method. The usefulness of the approach is illustrated by two application examples: a granulation process with particle aggregation and a crystallisation process with particle growth and complex fluid dynamics.

Keywords: particulate processing; distributed parameter systems; nonlinear systems; model reduction; population balance system; proper orthogonal decomposition; crystallisation; granulation

1. INTRODUCTION

Particulate processes play an important role in chemical and pharmaceutical industry. The majority of products in these areas are in the form of particles. Crystallisation, granulation or polymerisation are prominent examples for particulate processes.

Particulate processes typically consist of a fluid phase and a particle phase. The fluid phase is described accurately by the Navier Stokes equations in up to three space dimensions. To describe the particle phase, population balance equations have been widely accepted as an adequate tool (Ramkrishna, 2000). Population balances typically are partial differential equations, whose independent variables are the time and one or several characteristic particle properties like the characteristic particle size or the particle composition. An important difference between population balance systems and spatially distributed systems is that the interaction between two points in space usually decreases with their distance, whereas in population balances strong interactions may occur between remote points on the property coordinate. Examples are breakage phenomena, where a larger particle breaks into several smaller ones, or agglomeration phenomena, where two small particles merge to a larger one. Agglomeration and breakage cause integral terms in the population balances and turn the population balances into partial integro-differential equations.

The numerical treatment of coupled systems of Navier Stokes equations and population balances is challenging (John et al., 2009). Further, the complicated structure of the equations makes it hard to apply them to the solution of process control problems as it limits the number of applicable controller design techniques. Therefore, process control tasks require reduced model formulations.

External coordinates often reduced by simplifying assumptions like perfect mixing or compartment models. The weakness of such heuristic approaches is that they may give quite poor results when the flow conditions or the process geometry change. The method of moments and its extensions are frequently used to reduce population balance equations to low order model systems (Marchisio et al., 2003). Although well developed, it may be seen as a certain drawback of the method that the resulting reduced model only describes the moments of a particle distribution, but not the distribution itself. To obtain reduced models of industrial particulate processes, a more systematic method is desirable that reduces both external and internal coordinates. The use of proper orthogonal decomposition (POD) seems to be a promising approach. The key idea is to approximate the property distributions by a linear combination of problem specific basis functions, which are computed from solutions of the detailed reference model. The method requires test simulations with the detailed model to generate the basis functions and further coefficients of the reduced model. This preparation step may be computationally quite expensive, but as a reward one obtains a nonlinear reduced model of low order that can be solved quite easily.

In this contribution, two examples are used to illustrate the reduction method. The first example is a model of a granulation process. The main challenge is to treat the

integral term in the population balance, which results from particle aggregation. The example is also used to outline the reduction method. The second example is a laboratory scale crystalliser for the production of urea crystals. The process is growth dominated and the influence of the fluid flow is taken into account. This leads to a system with two external and one internal coordinate. For the model reduction by POD, a special difficulty arises from the nonlinearity of the growth term. This nonlinearity complicates the solution of integrals appearing when applying Galerkin's method of weighted residuals. Best point interpolation (Nguyen et al., 2008) is found to be a good solution for this problem.

2. MODEL REDUCTION FOR A DRUM GRANULATOR

Granulation is a technique used to enlarge particles by mixing them with a liquid, the binder, that agglomerates smaller particles to larger units. Granulation is often done in rotating drums containing the solid. In batch operation, a powder of fine particles is filled into the drum at the beginning of the process. During the process, liquid binder is added at a certain defined spray rate. How to change the binder spray rate over time in order to get particles with desired properties is a major design problem for this type of process.

2.1 Reference model

The following work is based on a dynamic model of a drum granulator published by Wang et al. (2006). In the variant used here, the model assumes perfect mixing inside the drum, i.e. it is space independent. The particle mass density distributions are described as a function of the time and a characteristic particle size. The main physical phenomena accounted for are particle growth and particle agglomeration. The model consists of a population balance for the solid particle, a balance for the powder mass, and a balance for the liquid content of the drum. The balance equations are listed in the following.

- The population balance for the particle mass density distribution $m(L,t)$, where L is the characteristic particle size, reads:

$$\begin{aligned}\frac{\partial m}{\partial t} &= -L^3\frac{\partial}{\partial L}\left(G\frac{m}{L^3}\right)\\ &+\frac{L^5}{2}\int_{L_{min}}^{L}\frac{6}{\pi\rho}\frac{\beta\left(\left(L^3-\lambda^3\right)^{\frac{1}{3}},\lambda\right)}{\left(L^3-\lambda^3\right)^{\frac{2}{3}}}\\ &\qquad\frac{m\left(\left(L^3-\lambda^3\right)^{\frac{1}{3}},t\right)}{L^3-\lambda^3}\frac{m(\lambda),t}{\lambda^3}d\lambda\\ &-m(L,t)\frac{6}{\pi\rho}\int_{L_{min}}^{L_{max}}\beta(L,\lambda)\frac{m(\lambda,t)}{\lambda^3}d\lambda \qquad (1)\end{aligned}$$

  The first term on the right hand side of (1) describes particle growth with a growth rate G, which is size independent and a function of the powder mass and the liquid content. The second and the third term describe changes in the particle mass distribution due to agglomeration; β is the coalescence kernel given by

$$\beta = \beta_0(x_w)\frac{(L+\lambda)^2}{L\,\lambda} \qquad (2)$$

  For the precise definition of G and β_0 see (Wang et al., 2006).
- The particle growth causes a mass transfer from the fine powder to the particle phase. The balance for the fine powder mass M_{powder} reads

$$\frac{dM_{powder}}{dt} = \int_{L_{min}}^{L_{max}} L^3\frac{\partial}{\partial L}\left(G\frac{m}{L^3}\right)dL \qquad (3)$$

- A differential equation for the liquid content x_w follows from the liquid mass balance:

$$M_{total}\frac{dx_w}{dt} = R_w \qquad (4)$$

  In (4) $M_{total} = \int_{L_{min}}^{L_{max}} m(L,t)dL + M_{powder}$ is the total solid mass, and R_w is the binder spray rate.

To solve the reference equations numerically, the mass conserving discretisation scheme by Litster et al. (1995) with $i_{max} = 20$ size intervals and $q = 4$ internal discretisations per size interval is used.

2.2 Model Reduction

The technique of proper orthogonal decomposition (POD) (Sirovich, 1987; Park and Cho, 1996; Kunisch and Volkwein, 2003) is applied to obtain a reduced model. As a first step, the particle mass density function is expressed by the series approach

$$m(L,t) \approx \sum_{i=1}^{N}\mu_i(t)\psi_i(L) \qquad (5)$$

The space dependent basis functions $\psi_i(L)$ are computed from test simulations with the reference model. Differential equations for the time dependent functions $\mu_i(t)$ are obtained from Galerkin's method of weighted residuals. Both steps are explained in the following.

Generation of basis functions Proper orthogonal decomposition uses problem specific basis functions. A set of orthonormal basis functions is generated from test simulations with the reference model, so-called snapshots. In the drum granulator example, the snapshots are dynamic solutions of the particle mass density distribution $m(L,t)$ at N_s time points $t_1,\ldots,t_{N_s}$. The basis functions are chosen in such a way that they approximate the average of the snapshots in a best possible way. This can be formulated as the optimisation problem for a basis function $\psi_j(L)$:

$$\begin{aligned}&\sum_{s=1}^{N_s}\big(m(L,t_s) - (m(L,t_s),\psi_j(L))_\Omega\,\psi_j(L),\\ &\qquad m(L,t_s) - (m(L,t_s),\psi_j(L))_\Omega\,\psi_j(L)\big)_\Omega \stackrel{!}{=} \min \qquad (6)\end{aligned}$$

The brackets $(.,.)_\Omega$ denote the scalar product:

$$(f(L),g(L))_\Omega = \int_{L_{min}}^{L_{max}} f(L)\;g(L)\;dL \qquad (7)$$

The term $(m(L,t_s),\psi_j(L))_\Omega = \mu_j(t_s)$ is the projection of the snapshot $m(L,t_s)$ on $\psi_j(L)$. The optimisation problem (6) is constrained by the scaling condition

$$(\psi_j(L),\psi_j(L))_\Omega = 1 \qquad (8)$$

When expressing the basis functions by

$$\psi_j(L) = \sum_{s=1}^{N_s} m(L, t_s)\, v_{sj} \tag{9}$$

with still unknown coefficients v_{sj}, it can be shown that the optimisation problem (6, 8) may be transformed into the eigenvalue problem

$$\underbrace{\begin{pmatrix} M_{11} & M_{12} & \cdots & M_{1N_s} \\ M_{21} & M_{22} & \cdots & M_{2N_s} \\ \vdots & \ddots & & \vdots \\ M_{N_s1} & M_{N_s2} & \cdots & M_{N_sN_s} \end{pmatrix}}_{=:\boldsymbol{M}} \underbrace{\begin{pmatrix} v_{1j} \\ v_{2j} \\ \vdots \\ v_{N_sj} \end{pmatrix}}_{=:\boldsymbol{v}_j} = \lambda_j \begin{pmatrix} v_{1j} \\ v_{2j} \\ \vdots \\ v_{N_sj} \end{pmatrix} \tag{10}$$

where M_{ij} is the abbreviation for the scalar product of two snapshots:

$$M_{ij} = (m(L, t_i), m(L, t_j))_\Omega \tag{11}$$

As $\boldsymbol{M}$ is symmetric, the eigenvectors $\boldsymbol{v}_j$ are orthogonal. It is easy to show that therefore the basis functions are orthogonal, as well, i.e.

$$(\psi_j(L), \psi_k(L))_\Omega = 0 \text{ for } j \neq k \tag{12}$$

The eigenvalues λ_j may be interpreted as a measure for how relevant the basis function ψ_j is for the reproduction of the snapshots (Holmes et al., 1998). A small value of λ_j means that the corresponding basis function does not contribute significantly to the approximation of the snapshots and may be neglected. In this sense the eigenvalues of $\boldsymbol{M}$ help to choose an appropriate number N of basis functions in the series approximation (5) for $m(L, t)$.

In summary, the computation of basis functions requires (i) the generation of N_s snapshots, (ii) the generation of the $N_s \times N_s$ matrix $\boldsymbol{M}$ and (iii) the solution of the eigenvalue problem (10). Especially the first step may computationally expensive if the reference model is complex. However, one should note that the computation time needed to generate the basis functions does not increase the computation time for the solution of the reduced model, as the basis functions are generated before solving the reduced model.

For illustration, Figure 1 shows the first three basis functions of the drum granulator problem.

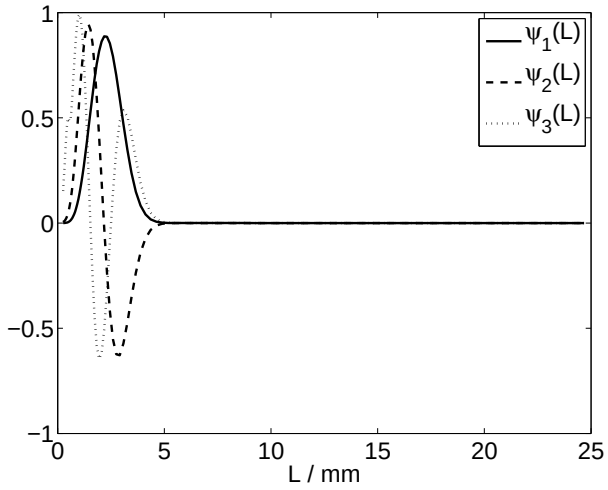

Fig. 1. First three basis functions of the reduced drum granulator model

Derivation of reduced model equations In order to obtain differential equations for the time dependent functions $\mu_j(t)$ in the series expression (5), the method of weighted residuals is applied. It is requested that, when inserting the approximation (5) for $m(L, t)$ into the population balance (1), the projection of the residual on the basis functions should vanish, i.e.

$$\begin{aligned}
\left(\frac{\partial m}{\partial t}, \psi_j\right)_\Omega &= -\left(L^3 \frac{\partial}{\partial L}\left(G \frac{m}{L^3}\right), \psi_j\right)_\Omega \\
&+ \left(\frac{L^5}{2} \int_{L_{min}}^{L} \frac{6}{\pi\rho} \frac{\beta\left(\left(L^3 - \lambda^3\right)^{\frac{1}{3}}, \lambda\right)}{\left(L^3 - \lambda^3\right)^{\frac{2}{3}}} \right. \\
&\qquad \left. \frac{m\left(\left(L^3 - \lambda^3\right)^{\frac{1}{3}}, t\right)}{L^3 - \lambda^3} \frac{m(\lambda), t}{\lambda^3} d\lambda,\ \psi_j \right)_\Omega \\
&- \left(m(L, t) \frac{6}{\pi\rho} \int_{L_{min}}^{L_{max}} \beta(L, \lambda) \frac{m(\lambda, t)}{\lambda^3} d\lambda,\ \psi_j\right)_\Omega \\
&\qquad\qquad (j = 1, \ldots, N)
\end{aligned} \tag{13}$$

The terms in (13) may be rearranged in the following way:

$$\left(\frac{\partial m}{\partial t}, \psi_j\right)_\Omega = \frac{d\mu_j}{dt} \tag{14}$$

$$\left(L^3 \frac{\partial}{\partial L}\left(G \frac{m}{L^3}\right), \psi_j\right)_\Omega = G \sum_{i=1}^{N} \mu_i \underbrace{\left(L^3 \frac{\partial}{\partial L}\left(\frac{\psi_i}{L^3}\right), \psi_j\right)_\Omega}_{=:\, A_{ji}} \tag{15}$$

$$\left(\frac{L^5}{2} \int_{L_{min}}^{L} \frac{6}{\pi\rho} \frac{\beta\left(\left(L^3-\lambda^3\right)^{\frac{1}{3}}, \lambda\right)}{\left(L^3-\lambda^3\right)^{\frac{2}{3}}} \frac{m\left(\left(L^3-\lambda^3\right)^{\frac{1}{3}}, t\right)}{L^3-\lambda^3} \frac{m(\lambda),t}{\lambda^3} d\lambda,\ \psi_j \right)_\Omega$$
$$= \sum_{i=1}^{N}\sum_{k=1}^{N} \frac{6}{\pi\rho}\, \beta_0(x_w)\, \mu_i(t)\, \mu_k(t)$$

$$\underbrace{\int_{L=L_{min}}^{L_{max}} \int_{\lambda=L_{min}}^{L} \frac{L^5}{2\left(L^3-\lambda^3\right)^{\frac{2}{3}}} \frac{\left(\left(L^3-\lambda^3\right)^{\frac{1}{3}}+\lambda\right)^2}{\left(L^3-\lambda^3\right)^{\frac{4}{3}}\lambda^4} \psi_i\left(\left(L^3-\lambda^3\right)^{\frac{1}{3}}\right) \psi_k(\lambda)\, d\lambda\, \psi_j(L)\, dL}_{=:\, B'_{jki}} \quad (16)$$

$$\left(m(L,t) \frac{6}{\pi\rho} \int_{L_{min}}^{L_{max}} \beta(L,\lambda) \frac{m(\lambda,t)}{\lambda^3} d\lambda,\ \psi_j \right)_\Omega$$
$$= \sum_{i=1}^{N}\sum_{k=1}^{N} \frac{6}{\pi\rho}\, \beta_0(x_w)\, \mu_i(t)\, \mu_k(t)$$

$$\underbrace{\int_{L=L_{min}}^{L_{max}} \psi_i(L)\, \psi_j(L) \int_{\lambda=L_{min}}^{L_{max}} \frac{(L+\lambda)^2}{L\,\lambda^4} \psi_k(\lambda)\, d\lambda\, dL}_{=:\, B''_{jki}} \quad (17)$$

Inserting the approximation (5) for $m(L,t)$ into the powder mass balance (3) gives

$$\frac{dM_{powder}}{dt} = G \sum_{i=1}^{N} \mu_i(t) \underbrace{\int_{L_{min}}^{L_{max}} L^3 \frac{\partial}{\partial L}\left(\frac{\psi_i}{L^3}\right)}_{=:\, C_i} \quad (18)$$

The coefficients A_{ji}, B'_{jki}, B''_{jki} and C_i have to be computed by numerical quadrature, which may be quite expensive. However, as the integrals depend only on the basis functions, the quadratures can be done offline, before the runtime of the reduced model. Therefore, their computation does not slow down the solution of the reduced model. For the reduced model, A_{ji}, B'_{jki}, B''_{jki} and C_i are just constant parameters.

Solution of the reduced model During runtime of the reduced model, the following set of ordinary differential equations has to be solved ($j = 1, \ldots, N$):

$$\frac{d\mu_i}{dt} = -G \sum_{i=1}^{N} A_{ji}\, \mu_i + \frac{6}{\pi\rho}\, \beta_0(x_w) \sum_{i=1}^{N}\sum_{k=1}^{N} (B'_{jki} - B''_{jki})\, \mu_i\, \mu_k \quad (19)$$

$$\frac{dM_{powder}}{dt} = G \sum_{i=1}^{N} C_i\, \mu_i \quad (20)$$

$$M_{total} \frac{dx_w}{dt} = R_w \quad (21)$$

One can see that the reduced model system has a nice and simple structure with a sum of quadratic terms that replaces the integrals appearing in the original population balance (1). It is found that $N = 6$ basis functions approximate the particle mass density distribution sufficiently well, so the reduced model consists of eight differential equations.

A test simulation compares the reduced model and the reference. In the test, binder is added for the first 33 s. Figure 2 shows the resulting size distributions. One can see that there is a good agreement between the reduced model and the reference solution.

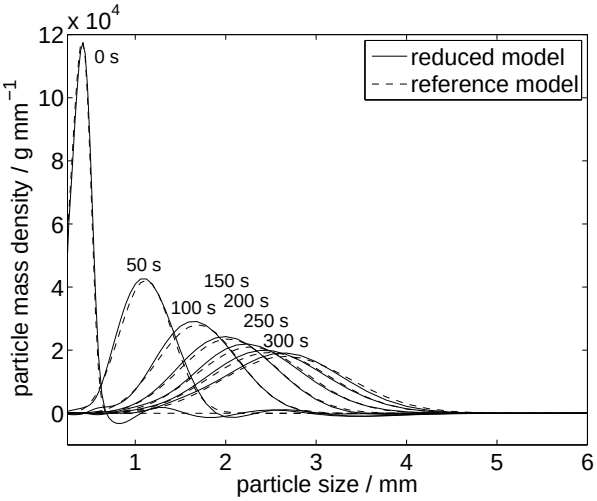

Fig. 2. Mass density distributions resulting when binder is added at the beginning of the batch process only.

In literature, it has been seen as a drawback of spectral methods like the POD method applied here that these methods are not mass conservative (Bück et al., 2011). In principle, this is true. However, in contrast to non-mass-conservative discretisation schemes, the variation of the total mass in this case is not a numerical inaccuracy, but lies in the nature of the projection method. This is illustrated by Figure 3, which shows the total mass of the particles when projected on the subspace defined by the basis functions. Although the total mass is constant in the reference simulation due to the mass conservative discretization scheme, the *projected* total mass in the reference simulation varies with time. This variation is reproduced by the reduced model with quite good accuracy.

In conclusion, the reduced model seems to describe the drum granulation process with sufficient accuracy to be applicable to control problems.

3. MODEL REDUCTION FOR A UREA CRYSTALLISER

Crystallisation is widely used in chemical industry, not only to produce crystalline substances, but also to separate mixtures or purify products. A a urea crystalliser is taken as an example for this process class. Urea is an organic chemical with many applications, like in fertilisers, in cosmetics, or for the selective catalytic reduction of NO_x in exhaust gases from diesel engines.

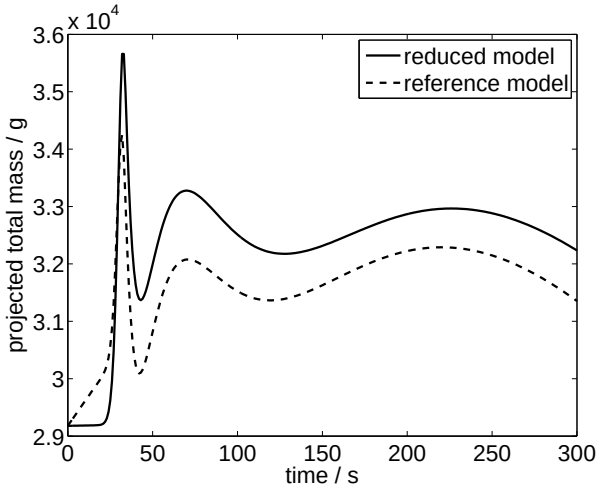

Fig. 3. Total mass of the particle distribution, when projected on the basis functions.

3.1 Reference model

A crystalliser consisting of a tube with a rectangular cross section is considered (see Figure 4). A reference model

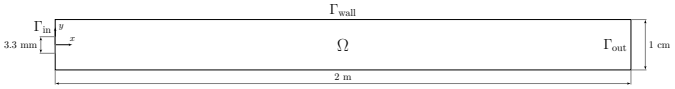

Fig. 4. Geometry of a laboratory urea crystalliser

for this process was developed in previous publications (Krasnyk et al., 2011a,b) and is briefly presented here. As the dynamics of the fluid flow reach the steady state much faster than those of the energy balance and the population balance for the considered data, a stationary fluid flow is assumed. Further, the fluid phase is modelled as incompressible, and the inlet velocity is a fully developed laminar flow. With these assumptions, the fluid flow in the crystalliser is described by the incompressible stationary Navier-Stokes equations:

$$\nabla \cdot \mathbf{u} = 0, \qquad \rho(\mathbf{u} \cdot \nabla)\mathbf{u} + \nabla p = \mu_{\mathrm{E}} \Delta \mathbf{u} \qquad \text{in } \Omega, \quad (22)$$

where $\mathbf{u} = \{u,\ v\}$ is the fluid velocity, p is the pressure, μ_{E} and ρ are the viscosity and the density of the fluid, respectively.

The energy balance leads to a differential equation for the temperature T that reads

$$\rho c_p \left(\frac{\partial T}{\partial t} + \mathbf{u} \cdot \nabla T \right) = \lambda_{\mathrm{E}} \Delta T + \Delta H_{\mathrm{cryst}} \cdot h_{\mathrm{gr}}, \qquad \text{in } (0, T] \times \Omega \quad (23)$$

where c_p and λ_{E} are the heat capacity and the thermal conductivity of ethanol, and $\Delta H_{\mathrm{cryst}}$ is the heat of solution.

A component mass balance for the solute gives the following convection-diffusion equation for the solute partial density ρ_c:

$$\frac{\partial \rho_c}{\partial t} + \mathbf{u} \cdot \nabla \rho_c = D_c \Delta \rho_c + h_{\mathrm{gr}}, \qquad \text{in } (0, T] \times \Omega \quad (24)$$

where D_c is the diffusion coefficient. The term h_{gr} stands for the mass transfer between fluid phase and particle phase due to crystal growth. It can be written as

$$h_{\mathrm{gr}}(T, \rho_c, f) = -3 \rho_d k_V G(T, \rho_c) \int_0^\infty L^2 f dL, \quad (25)$$

where ρ_d is the density of the crystals, G is the growth rate of crystals, and f is the number density function of the crystal population.

The dispersed particle phase is modelled by a population balance for the particle size distribution that accounts for crystal growth and convective transport of crystals in space:

$$\frac{\partial f}{\partial t} + \mathbf{u} \cdot \nabla f + G \frac{\partial f}{\partial L} = D_f \Delta f, \qquad \text{in } (0, T] \times \Omega \times [0, \infty) \quad (26)$$

here D_f is an artificial diffusion coefficient of particles in the solute which describes a movement of the particles relative to the fluid flow. It is mainly introduced to increase numerical robustness. The particle size distribution f depends not only on time and space, and in addition it also depends on the particle size coordinate L.

A power function is used for the growth rate:

$$G = \begin{cases} k_g \sigma(T, \rho_c)^g, & \sigma > 0, \\ 0, & \sigma \leq 0, \end{cases} \quad (27)$$

where σ is the super-saturation defined as

$$\sigma(T, \rho_c) = \frac{\rho_c - \rho_{c,sat}(T)}{\rho_{c,sat}(T)}, \quad (28)$$

with an empirical expression for the saturation density $\rho_{c,sat}(T)$.

3.2 Model reduction

The development of a reduced model for the urea crystalliser model has been described before (Krasnyk et al., 2011b) and is not repeated here in detail. Most of the reduction steps are analogous to the drum granulator example. However, additional difficulties arise due to the nonlinear particle growth rate. This nonlinearity causes the weighted residuals of the model equations to contain integrals that depend on the states of the reduced model in a nonlinear way. An analytical solution of these integrals is not possible. A solution by numerical quadrature is not satisfactory either, as it would increase the computation time of the reduced model considerably. There is a need for an efficient approximation method that generates low computational costs during the runtime of the reduced model. Such an approximation may be the best point interpolation by Nguyen et al. (2008).

The idea us to approximate the growth rate $G(T, \rho_c)$ by a series expression, analogous to the approximation of the system states:

$$G(T, \rho_c) \approx \sum_{i=1}^{N_G} \gamma_i(t)\ \psi_G(\boldsymbol{x}), \quad (29)$$

where $\boldsymbol{x}$ are the space coordinates. The basis functions $\psi_G(\boldsymbol{x})$ are constructed from snapshots in the same way as the basis functions for the system states. The coefficients γ_i follow from equating the series approximation with the nonlinearity at certain interpolation points $\mathbf{x}_m$:

$$\sum_{i=1}^{N_G} \gamma_i(t)\ \psi_G(\mathbf{x}_m) = G(T(\mathbf{x}_m), \rho_c(\mathbf{x}_m)), \quad m = 1, \ldots, N_G. \quad (30)$$

The interpolation points $\mathbf{x}_m$ are chosen such that the approximation error is minimised in some sense. The choice is made in an offline optimisation step that precedes the solution of the reduced model. During run time of the reduced model, the interpolation points are not changed.

The big advantage of the best point interpolation is that when inserting the approximation (29) into the integrals in the weighted residuals, one obtains integral terms that depend on the basis functions only and that may be evaluated offline, during the generation of the reduced model. At run time of the reduced model, no more numerical quadrature is required. Instead, one only has to evaluate the nonlinear function G at N^G points and one has to solve N_G linear equations (30).

Figure 5 shows a test simulation with the reduced model. The wall temperature as the main manipulating variable in this process is varied. The figure shows the conditions at the crystalliser outlet, as these determine the product quality. One can see that there is a nearly perfect match between the temperatures of the reduced model and the reference model, and that there is a good agreement between the crystal size distributions.

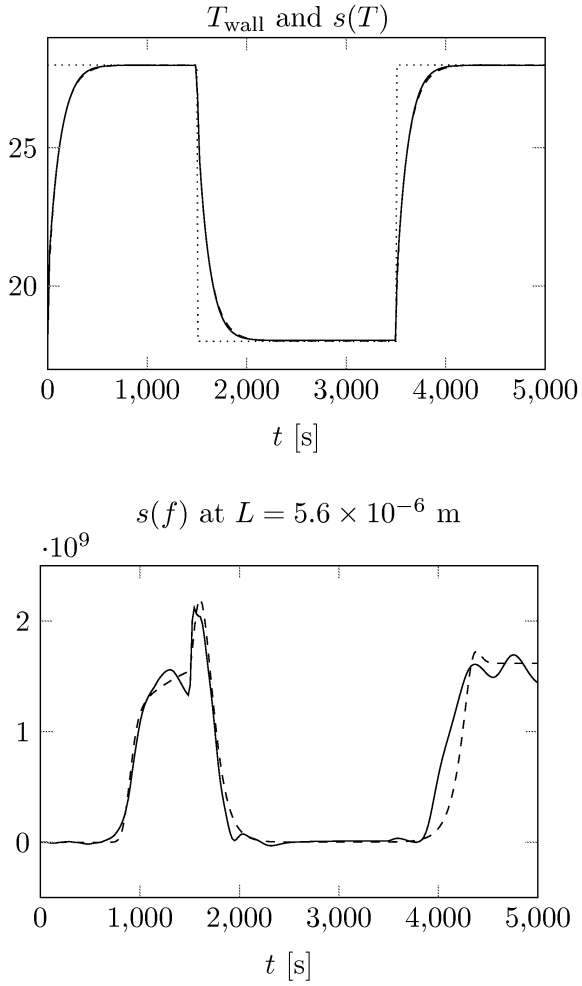

Fig. 5. Comparison between reference model and reduced model of the urea crystalliser for step changes in the wall temperature; crystalliser temperature and number density function for a certain crystal size are shown; $s(.)$ denotes an averaging over the crystalliser outlet.

REFERENCES

Bück, A., Klaunick, G., Kumar, J., M., P., and Tsotsas, E. (2011). Numerical simulation of particulate processes for control and estimation by spectral methods. *AIChE Journal (in press, available online)*. doi: 10.1002/aic.12757.

Holmes, P., Lumley, J., and Berkooz, G. (1998). *Turbulence, Coherent Structures, Dynamical Systems and Symmetry*. Cambridge University Press.

John, V., Roland, M., Mitkova, T., Sundmacher, K., Voigt, A., and Tobiska, L. (2009). Simulations of population balance systems with one internal coordinate using finite element methods. *Chemical Engineering Science*, 64(4), 733–741.

Krasnyk, M., Borchert, C., and Mangold, M. (2011a). Model reduction techniques for the simulation of particle populations in fluid flow. *Mathematical and Computer Modelling of Dynamical Systems (accepted)*.

Krasnyk, M., Mangold, M., Ganesan, S., and Tobiska, L. (2011b). Reduction of a crystallizer model with internal and external coordinates by proper orthogonal decomposition. *Chemical Engineering Science (accepted)*.

Kunisch, K. and Volkwein, S. (2003). Galerkin proper orthogonal decomposition methods for a general equation in fluid dynamics. *SIAM Journal on Numerical Analysis*, 40, 492–515.

Litster, J., Smit, D., and Hounslow, M. (1995). Adjustable discretized population balance for growth and aggregation. *AIChE Journal*, 41, 591–603.

Marchisio, D., Vigil, R., and Fox, R. (2003). Implementation of the quadrature method of moments in CFD codes for aggregation-breakage problems. *Chemical Engineering Science*, 58, 3337–3351.

Nguyen, N.C., Patera, A.T., and Peraire, J. (2008). A "best points" interpolation method for efficient approximation of parametrized functions. *International Journal for Numerical Methods in Engineering*, 73(4), 521–543. doi:10.1002/nme.2086. URL `http://dx.doi.org/10.1002/nme.2086`.

Park, H. and Cho, D. (1996). The use of the karhunen-loève decomposition for the modeling of distributed parameter systems. *Chemical Engineering Science*, 51, 81–98.

Ramkrishna, D. (2000). *Population balances: theory and applications to particulate systems in engineering*. Academic Press.

Sirovich, L. (1987). Turbulence and the dynamics of coherentstructures. Part 1: coherent structures. *Quarterly of Applied Mathematics*, 45, 561–571.

Wang, F., Ge, X., Balliu, N., and Cameron, I. (2006). Optimal control and operation of drum granulation processes. *Chemical Engineering Science*, 61, 257–267.